Catalysis Communications 115 (2018) 17–20

Contents lists available at ScienceDirect

Catalysis Communications

journal homepage: www.elsevier.com/locate/catcom

Short Communication

# Oxygen reduction reaction on $M_3$(hexaiminobenzene)$_2$: A density function theory study

Xuejing Yang, Qiang Hu, Xiuli Hou*, Jianli Mi, Peng Zhang*

*Institute for Advanced Materials, School of Materials Science and Engineering, Jiangsu University, Zhenjiang 212013, China*

ARTICLE INFO

*Keywords:*
Oxygen reduction reaction
$M_3$(hexaiminobenzen)$_2$
Density functional theory
Electrocatalysis

ABSTRACT

In this work, density functional theory calculations have been performed to investigate the catalytic activity of $M_3(HIB)_2$ complex nanosheets for the oxygen reduction reaction (ORR), where HIB is hexaiminobenzene and M denotes Fe, Os, Ir or Pt. The results showed that the ORR activity of $M_3(HIB)_2$ is closely related to the selection of the central metal atom. The value of the overpotential increases in the order: $Ir_3(HIB)_2 < Fe_3(HIB)_2 < Pt_3(HIB)_2 < Os_3(HIB)_2$. Due to its optimum adsorption strength and the smallest value of overpotential, the $Ir_3(HIB)_2$ nanosheet exhibits the best ORR catalytic activity among the four $M_3(HIB)_2$ nanosheets. The results of this work provide important fundamental insight for this class of nanosheets materials for the ORR in polymer electrolyte fuel cells.

## 1. Introduction

In recent times, polymer electrolyte fuel cells (PEFCs) have attracted a great deal of interest as promising candidates for applications pertaining to sustainable and efficient power production. However, the low rate of the oxygen reduction reaction (ORR) at the cathode in PEFCs continues to be a major technical challenge. At present, Pt and Pt-based materials are widely employed as cathode materials for ORR [1, 2]. However, their high cost, scarce availability and short durability hinders a broad range of commercial applications of PEFCs. Therefore, it is meaningful to explore cost-effective and high durability catalysts for ORR purposes, such as transition metal oxides [3], core-shell nanoparticles [4], metal-free heteroatom doped carbon materials [5] and transition metal − nitrogen − carbon catalysts (TM-$N_x$/C) [6, 7].

TM-$N_x$/C catalysts have been extensively studied due to their low cost and very high catalytic efficiency. Previous studies have shown that varying the central transition metal atom would affect the adsorption energies of the intermediates generated from ORR processes [8, 9]. It has been proven that the $FeN_x$/C catalyst possesses high activity towards ORR [10, 11], and that the prime active sites are the Fe-$N_4$ moieties [12, 13]. Moreover, the catalytic performance of $FeN_x$/C catalysts can be comparable or even better than that of Pt (111) surface in alkaline media [13, 14]. In the same way, Co-$N_x$/C electrocatalyst also exhibits high efficiency and stability in alkaline or acidic solutions [13, 15]. In a previous work, Yuasa et al. [16] have reported that the ORR active-site in the structure of Co-$N_x$/C is $CoN_4$, while Bashyam et al. [17] attributed the catalytic activity to $CoN_2$ moiety. Kattel et al. [15] applied density functional theory (DFT) calculations to demonstrate that $CoN_4$ defect is the dominant active site in Co-$N_x$/C catalysts. In addition, Kattel et al. [18] studied the Ni-$N_x$-C ORR electrocatalysts and found that the Ni − $N_2$ edge site exhibits good degree of catalytic performance in alkaline and acidic media, as opposed to the graphitic Ni − $N_2$ and Ni − $N_4$ sites. Recently, it was discovered that $Ni_3(HITP)_2$ (HITP = 2, 3, 6, 7, 10, 11- hexaiminotriphenylene) is a highly conductive two-dimensionally layered material [19], and subsequently Miner et al. [20] found that $Ni_3(HITP)_2$ containing Ni − $N_4$ sites exhibits high catalytic activity, which is competitive with most of the active non-platinum group metals in alkaline media. Recently, it has been confirmed that $M_3(HIB)_2$ (where HIB represents hexaiminobenzene and M denotes Ni and Cu), which has a structure similar to $Ni_3(HITP)_2$, also exhibits high conductivity [21]. However, no studies have been reported so far focusing on the ORR catalytic activity of $M_3(HIB)_2$, which will be considered in this work.

Previous studies implied that the structure and component of the active site is of crucial importance in improving the catalytic properties [22]. Based on the previous studies, a key issue determining the performance of ORR catalysts is the TM-$N_x$ structure embedded within graphene-based materials. At present, most of the research works focused on the Fe, Co, Ni-$N_x$ embedded graphene materials. Thus, an obvious question arises: is there any other metallic element that can act as the central atom and exhibit high catalytic activity?

In this work, we take $M_3(HIB)_2$ nanosheets (M denotes Os, Ir or Pt) as examples to investigate the effect of the central element on their catalytic activity and compare it with $Fe_3(HIB)_2$. The adsorption strength of ORR intermediates and the catalytic activity of ORR are studied by DFT calculations. Subsequently, we plot a volcano curve to

* Corresponding authors.
*E-mail addresses:* houxiuli@ujs.edu.cn (X. Hou), zhangpjlxb@ujs.edu.cn (P. Zhang).

https://doi.org/10.1016/j.catcom.2018.06.022
Received 26 March 2018; Received in revised form 21 June 2018; Accepted 22 June 2018
Available online 26 June 2018

establish a definite relationship between them. In order to understand the different catalytic activity of the $M_3(HIB)_2$ nanosheet, the electronic structures are also calculated by DFT. Our results not only show that $Ir_3(HIB)_2$ nanosheets exhibit the best ORR catalytic activity among the four kinds of $M_3(HIB)_2$ nanosheets but also advocate the conclusion that the appropriate selection of a central metal atom is essential for optimizing the ORR activity of TM-$N_x$/C catalysts.

## 2. Computational methods

All calculations were performed based on the DMol$^3$ code [23]. The exchange-correlation potential was treated by the generalized gradient approximation (GGA) using the PW91 functional and the all electron relativistic method was employed for the core treatment [24]. Meanwhile, the double numerical atomic orbital plus polarization function (DNP) was adopted as the basic set. The smearing value of 0.005 Ha was used throughout the computational calculations. Because the density drops off quickly as the distance from an atomic nucleus increases, a real space global orbital cutoff radius of 5.2 Å was used to ensure highly reliable results. The convergence tolerance of energy, maximum force, and maximum displacement in the geometrical structural optimization has been obtained to be $1 \times 10^{-5}$ Ha, 0.002 Ha/Å, and 0.005 Å, respectively.

In this work, $M_3(HIB)_2$ nanosheets (M = Fe, Os, Ir, Pt) as possible ORR catalysts have been studied thoroughly (Fig. 1). $M_3(HIB)_2$ nanosheets and their mirror images are separated through a vacuum layer with a thickness of 18 Å to eliminate possible interactions. The optimized lattice constants for $Fe_3(HIB)_2$, $Os_3(HIB)_2$, $Ir_3(HIB)_2$, and $Pt_3(HIB)_2$ are $13.6 \times 13.6 \times 18.0$, $13.9 \times 13.9 \times 18.0$, $14.0 \times 14.0 \times 18.0$, and $13.9 \times 13.9 \times 18.0$ Å$^3$, respectively (Table S1 in ESI). The formation energies ($E_f$) of $M_3(HIB)_2$ nanosheets were calculated to quantify their stability. The $E_f$ was calculated as follows: $E_f = 2E_{HIB} - 6E_{H2} + 3E_M - E_{M3(HIB)2}$, where $E_{HIB}$, $E_{H2}$, $E_M$, $E_{M3(HIB)2}$ are the electronic energies of hexaaminobenzenes, hydrogen molecules, the metal atoms and the $M_3(HIB)_2$ nanosheets, respectively [25]. $M_3(HIB)_2$ can be considered as the product from hexaaminobenzene and metal ion [21]. The calculated positive $E_f$ values suggest that $M_3(HIB)_2$ nanosheet is energy more favorable than reactants (Table S2 in ESI). The values of adsorption energy ($E_{ad}$) corresponding to the ORR intermediates formed on these catalysts were calculated using the formula $E_{ad} = E_{mol} + E_{M3(HIB)2} - E_{mol\text{-}M3(HIB)2}$, where $E_{mol}$, $E_{M3(HIB)2}$ and $E_{mol\text{-}M3(HIB)2}$ represent the electronic energies of an isolated adsorbate molecule, the $M_3(HIB)_2$ nanosheet, and the adsorption system, respectively [26]. The electronic energies of isolated adsorbate molecule were calculated in the supercell of $M_3(HIB)_2$ with the same settings. In view of these definitions, a positive value of $E_{ad}$ is representative of an exothermic adsorption process.

The Gibbs free energy ($\Delta G$) of reaction corresponding to the elementary steps in ORR was calculated based on the computational hydrogen electrode (CHE) model [27]. The $\Delta G$ was calculated using the equation: $\Delta G = \Delta E + \Delta ZPE - T\Delta S + \Delta G_U + \Delta G_{pH}$, where $\Delta E$ is the reaction energy change, $\Delta ZPE$ is the change of zero point energy, $T$ is the temperature which has a value of 298.15 K, and $\Delta S$ represents the entropy change [28]. The well-established $H_2O$ solvent environment is described by the conductor-like screening model (COSMO), wherein the dielectric constant is 78.54 for the $H_2O$ solvent [29]. The chemical potential of a proton coupled with an electron ($H^+ + e^-$) in solution equals to half of the $H_2$ molecule. The free energy of $H_2O$ in solution could be obtained in gas phase at a pressure of 0.035 bar, which is the equilibrium vapor pressure of $H_2O$ at 298.15 K. The free energy of $O_2(g)$ was derived according to $G_{O2(g)} = 2G_{H2O(l)} - 2G_{H2} + 4.92$ eV, since the high-spin ground state of oxygen molecule is notoriously poorly described in DFT calculations. The temperature (T) of 298.15 K was used in all calculations [30].

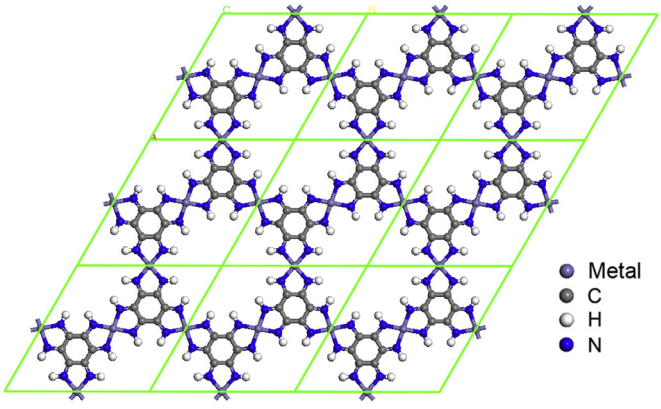


**Fig. 1.** Atomic structure of $M_3(HIB)_2$ nanosheet.

## 3. Results and discussion

The favorable adsorption properties of ORR intermediates are believed to be one of the necessary conditions for ensuring the smooth progress of the reaction [31]. The most stable adsorption structures of ORR intermediates ($O_2$, O, OH, and OOH) on $M_3(HIB)_2$ are depicted in Fig. S1 (ESI) and the corresponding $E_{ad}$ values are presented in Table S3 (ESI). The adsorption of $O_2$ on the electrode's surface is the first step in the progress of ORR, which usually determines the ORR catalytic active sites. Hence, it is necessary to study the adsorption characteristics of the $O_2$ molecule on $M_3(HIB)_2$. From Fig. S1 and Table S3 (ESI), it is obvious that $O_2$ prefers to adsorb on $Ir_3(HIB)_2$ with an end-on configuration, while the most energetically favorable configuration of $O_2$ on $Fe_3(HIB)_2$ and $Os_3(HIB)_2$ is characterized by a side-on configuration with $O_2$ molecules parallel to the surface of the catalysts and forming two chemical bonds with the Fe and Os atoms. Note that the $O_2$ molecule cannot adsorb on $Pt_3(HIB)_2$ with measurable surface concentration (extremely weak bonding), which may has a negative effect on the ORR. From Table S3 (ESI), the $E_{ad}$ value of $O_2$ decreases from 1.75 eV on $Fe_3(HIB)_2$ and 1.12 eV on $Os_3(HIB)_2$ to 0.49 eV on $Ir_3(HIB)_2$ and − 0.26 eV on $Pt_3(HIB)_2$, respectively.

Consistent with the characteristics of $O_2$ adsorption, other ORR intermediates prefer to be adsorbed at the top site of the central metal atom, and this is consistent with their adsorption properties on $FeN_4$/C and $CoN_4$/C [21, 22, 28]. Thus, we can conclude that the ORR active sites of $M_3(HIB)_2$ are also located on the top site of the central metal atom. It is found that the adsorption strength of OOH, O and OH on $M_3(HIB)_2$ also decreases with the increase in the electronegativity of the central metal atoms. Moreover, the desorption of $H_2O$ is favorable due to the physisorption of $H_2O$ molecule on the $Fe_3(HIB)_2$, $Ir_3(HIB)_2$ and $Pt_3(HIB)_2$, and the negative value of $E_{ad}$ corresponding to $H_2O$ adsorption on the $Os_3(HIB)_2$, which will facilitate the regeneration of the catalysts. The above results show that the central metal atom plays an important role in the adsorption of the ORR intermediates.

In order to investigate the origin of the interaction between the $O_2$ molecule and $M_3(HIB)_2$ nanosheet, the electronic structure of the $M_3(HIB)_2$ was investigated. It is well known that the surface electronic states of the catalyst determine the adsorption strength of the intermediates [17, 32]. Fig. S2 (ESI) illustrates the partial density of states (PDOS) of the central metal in the $M_3(HIB)_2$ nanosheets. The calculated d-band center values are obtained to be −2.82, −2.88 and − 4.20 eV for $Os_3(HIB)_2$, $Ir_3(HIB)_2$ and $Pt_3(HIB)_2$, respectively. It is obvious from Fig. S2 (ESI) that a left shift of the d-band from $Os_3(HIB)_2$ to $Pt_3(HIB)_2$, which suggests a downward shift relative to the Fermi level, which further results in a downward shift of the antibonding states and a tendency to cause a weaker adsorption of $O_2$ on the central metal atoms. In other words, the adsorption strength of $O_2$ decreases in the following order: $Os_3(HIB)_2$ > $Ir_3(HIB)_2$ > $Pt_3(HIB)_2$. This is consistent with the adsorption of all the ORR intermediates.

After the adsorption and activation of $O_2$, a four-electron ORR pathway occurs through the OOH association mechanism on the surface of Fe-$N_x$/C and Co-$N_x$/C catalysts in an acidic solution [14, 18, 29, 31].